International Geology Review
Publication details, including instructions for authors and subscription information:
http://www.tandfonline.com/loi/tigr20

Age and origin of a Palaeozoic nepheline syenite from northern Shanxi Province, China: U-Pb zircon age and whole-rock geochemical and Sr-Nd isotopic constraints

Shen Liu [a] , Ruizhong Hu [a] , Shan Gao [b] , Caixia Feng [a] , Ian M. Coulson [c] , Guangying Feng [a] , Yuhong Yang [a] , Youqiang Qi [a] , Chaogui Yang [a] & Liang Tang [a]

[a] State Key Laboratory of Ore Deposit Geochemistry , Institute of Geochemistry, Chinese Academy of Sciences , Guiyang , 550002 , PR China

[b] State Key Laboratory of Geological Processes and Mineral Resources , China University of Geosciences , Wuhan , 430074 , PR China

[c] Solid Earth Studies Laboratory, Department of Geology , University of Regina , Regina , SK , Canada , S4S 0A2

Published online: 16 Dec 2011.

International Geology Review
Vol. 54, No. 11, August 2012, 1296–1308

Age and origin of a Palaeozoic nepheline syenite from northern Shanxi Province, China: U–Pb zircon age and whole-rock geochemical and Sr–Nd isotopic constraints

Shen Liu[a]*, Ruizhong Hu[a], Shan Gao[b], Caixia Feng[a], Ian M. Coulson[c], Guangying Feng[a], Yuhong Yang[a], Youqiang Qi[a], Chaogui Yang[a] and Liang Tang[a]

[a]*State Key Laboratory of Ore Deposit Geochemistry, Institute of Geochemistry, Chinese Academy of Sciences, Guiyang 550002, PR China;* [b]*State Key Laboratory of Geological Processes and Mineral Resources, China University of Geosciences, Wuhan 430074, PR China;* [c]*Solid Earth Studies Laboratory, Department of Geology, University of Regina, Regina, SK, Canada S4S 0A2*

(*Accepted 24 October 2011*)

Geochronological, geochemical, and whole-rock Sr–Nd isotopic analyses were performed on a suite of Palaeozoic nepheline syenites from Zijinshan to characterize their ages and petrogenesis. Laser ablation inductively coupled plasma-mass spectrometry U–Pb zircon analyses yield consistent ages of 525.7 ± 2.8 million years for a sample (HYK01). These intrusive rocks belong to the foid syenite magma series in terms of $K_2O + Na_2O$ contents (14.3–15.2 wt.%) and to the shoshonitic series based on their high K_2O contents (5.42–5.61 wt.%). The nepheline syenites are further characterized by high light rare earth element contents [$(La/Yb)_N = 29.1–36.1$]; show modest negative Eu anomalies ($\delta Eu = 0.5–0.6$) and positive anomalies in Rb, Th, U, Pb, Zr, and Hf; are depleted in Ba and high field strength elements (P and Ti). In addition, all the nepheline syenites in this study display relatively low radiogenic Sr ($(^{87}Sr/^{86}Sr)_i$ (0.7042–0.7043) and positive ε_{Nd} (t) (0.7–0.8). These results suggest that the nepheline syenites were derived from depleted continental crust. The parent magmas likely experienced fractional crystallization of plagioclase, Ti-bearing oxides (e.g. rutile, ilmenite, and titanite), apatite, and zircon during ascent, with negligible crustal contamination before final emplacement at a high crustal level.

Keywords: nepheline syenites; petrogenesis; Palaeozoic; Shanxi Province; North China Craton

1. Introduction

Nepheline syenite is an alkaline rock that is similar in its medium- to coarse-grained appearance to granite. However, an essential compositional difference between the two rocks is that the nepheline syenite is deficient in silica and has a higher proportion of the alkalis sodium and potassium, as well as a higher proportion of alumina. Nepheline is a feldspathoid mineral of composition (Na, K) $AlSiO_4$ and usually forms small grains that are intercrystallized with feldspar. Its chemistry is close to alkali feldspars, but the latter are poorer in silica (Nepheline Syenite Inventory 1999; Tait *et al*. 2003). Compared with pure feldspars, advantages of the use of nepheline syenite include its high potassium and sodium content (K_2O + NaO is about 9–12% in feldspars whereas it is greater than 14% in nepheline syenite) and its generally lower melting temperature compared with potassium feldspar, which always contains other phases, such as quartz, that shift the melting point to higher temperatures (Esposito *et al*. 2005; Burat *et al*. 2006).

Nepheline syenite is often preferred in prospecting, plastics processes, glass technology, and paint and pottery processes, among others. There are over 12 nepheline syenite intrusions in China, six of which, including the studied alkaline rocks, are distributed in the North China Craton (NCC), five of which are spread in the Yangtze Craton, and one of which is found in the Tarim Craton (Huang and Qiu 2001). Their emplacements are strictly controlled by deep faults, such as the Panxi Rift in the Yangtze Craton and Xiaojiang and Nanpanjiang faults in other cratons. Most nepheline syenites were formed during the Yanshanian period, including the Gejiu intrusion (108.5–94.3 Ma), the Ningnan intrusion (206–193 Ma), the Zijinshan intrusion (138.7 Ma), the Yongping intrusion (>10 Ma), and the Fengcheng intrusion (166 Ma) (Huang and Qiu 2001). Few nepheline syenites formed during other times have been reported. As such, it is important to undertake detailed investigations of alkaline rocks, especially those alkaline associations within NCC.

Our work on ~526 Ma alkaline intrusions provides further insights into this debate and helps determine the

*Corresponding author. Email: liushen@vip.gyig.ac.cn

ISSN 0020-6814 print/ISSN 1938-2839 online

http://dx.doi.org/10.1080/00206814.2011.638436
http://www.tandfonline.com

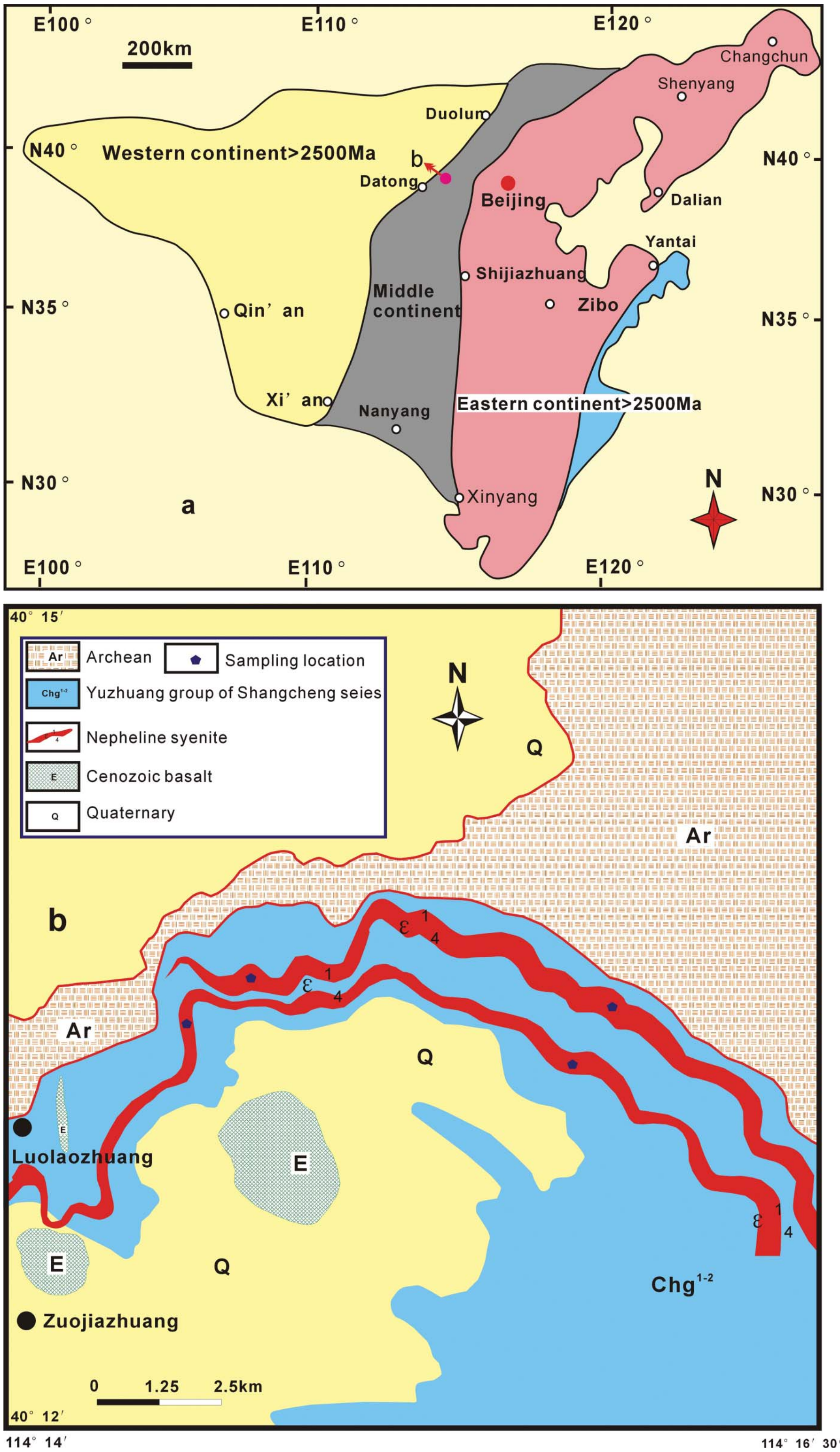

Figure 1. (A) Geological map of the study area, showing the three tectonic subdivisions of the North China Craton. (B) Distribution of nepheline syenite and the adjacent stratum in the Zijinshan area, Shanxi Province.

petrogenetic processes that occur during the later evolutionary stage. In this article, we present laser ablation inductively coupled plasma-mass spectrometry (LA-ICP-MS) U–Pb ages, major and trace element geochemistries, and Sr–Nd isotope data on the alkaline rocks of the nepheline syenite from the northern regions of Shanxi Province, China (Figure 1). These data are used to discuss the petrogenesis of these rocks.

2. Geological setting and petrography

There are over six nepheline syenite intrusions in the NCC (Huang and Qiu 2001); each of these alkaline rocks could provide important insights into the tectonothermal evolution of the lithosphere of the NCC, as well as possible palaeo-linkage(s) between the NCC and other craton(s). Many precise ages for the alkaline rocks in the NCC have been published in recent papers (Zhou and Zhao 1994, 1996; Zhao and Zhou 1994; Hu and Zhou 2007; Ying *et al*. 2007; Liu 2008; Yang *et al*. 2009), for example, the 135–125 Ma Zijinshan nepheline syenite in Shanxi Province, China.

The study area is located within Shanxi Province in the northern parts of the NCC (Figure 1A). Nepheline syenites in the study area are emplaced into the Yuzhuang group of the Shangcheng series stratum ($\boldsymbol{\varepsilon}^{1}{}_{4}$), and the alkaline rocks are near WE trending (Figure 1B). The alkaline rocks are commonly 150–630 m wide and 85–90 km in length. They are exposed for ~12.8–57.8 km^2. Representative pictures and photomicrographs of the nepheline syenites from the study area are provided in Figure 2. The alkaline rocks are all nepheline syenite with a granitic texture (Figure 2). The nepheline syenites appear grey and celadon, mainly containing 65–70% alkali feldspar (e.g. orthoclase, anorthoclase, feldspar, and albite), 16–25% nepheline (e.g. calcium nepheline), and 10–15% alkaline dark minerals (e.g. aegirine augite, aegirine, and arfvedsonite). Sometimes, the ring structure of pyroxene appears. Accessory minerals include magnetite, ilmenite, zircon, apatite, and titanite.

Figure 2. Representative photos and photomicrographs showing the sample and petrographic features of the nepheline syenites from Zijinshan. All samples display similar granitic textures.

3. Analytical methods

3.1. U–Pb dating by LA-ICP-MS

Zircon was separated from one sample (HYK01) using conventional heavy-liquid and magnetic techniques at the Langfang Regional Geological Survey, Hebei Province, China. Zircon separates were examined under transmitted and reflected light and by cathodoluminescence petrography at the State Key Laboratory of Continental Dynamics, Northwest University, China, to reveal their external and internal structures.

Laser ablation techniques were employed for zircon age determinations (Table 1; Figure 3) using an Agilent 7500a ICP-MS instrument equipped with a 193 nm excimer laser, housed at the State Key Laboratory of Geological Processes and Mineral Resources, China University of Geoscience, Wuhan, China. Zircon #91500 was used as a standard and NIST 610 was used to optimize the results. A spot diameter of 24 μm was used. Prior to LA-ICP-MS zircon U–Pb dating, the surfaces of the grain mounts were washed in dilute HNO_3 and pure alcohol to remove any potential lead contamination. The analytical methodology is described in detail by Yuan *et al.* (2004). Correction for common Pb was made following Andersen (2002). Data were processed using the GLITTER and ISOPLOT programs (Ludwig 2003) (Table 1; Figure 3). Errors for individual analyses by LA-ICP-MS are quoted at the 95% (1σ) confidence level.

3.2. Whole-rock major and trace elements, and Sr–Nd isotopes

Fifteen samples were collected for analyses of whole-rock major and trace elements, and 15 samples for Sr–Nd isotopes. Samples were trimmed to remove altered surfaces, cleaned with deionized water, crushed, and powdered in an agate mill.

Major elements were analysed with a PANalytical Axios-advance (Axios PW4400) X-ray fluorescence spectrometer at the State Key Laboratory of Ore Deposit Geochemistry, Institute of Geochemistry, Chinese Academy of Sciences (CAS), Guiyang. Fused glass discs were prepared for analyses of major elements. Analytical precision, as determined for the Chinese National Standards GSR-1 and GSR-3, was better than 5% for all elements (Table 2). Loss on ignition was obtained using 1 g of powder heated to 1100°C for 1 h.

Trace elements were measured using a Perkin–Elmer Sciex ELAN 6000 ICP-MS at the State Key Laboratory of Ore Deposit Geochemistry, Institute of Geochemistry, CAS, Guiyang. Powdered samples (50 mg) were dissolved in high-pressure Teflon bombs using a mixture of HF + HNO_3 and heated for 48 h at ~190°C (Qi *et al*. 2000). Rh was used as an internal standard to monitor signal drift during counting. Analyses of the international standard

Table 1. LA-ICP-MS U–Pb isotopic data for zircon within the nepheline syenites from Zijinshan, Shanxi Province.

Hyk 01	Isotopic ratios										Age (MA)					
Spot	Th(ppm)	U(ppm)	Pb(ppm)	Th/U	$^{207}Pb/^{206}Pb$	1σ	$^{207}Pb/^{235}U$	1σ	$^{206}Pb/^{238}U$	1σ	$^{207}Pb/^{206}$	1σ	$^{207}Pb/^{235}U$	1σ	$^{206}Pb/^{238}U$	1σ
1	979	2113	204	2.16	0.0557	0.0014	0.6750	0.0153	0.041	0.0009	517	32	524	9	520	5
2	367	881	87.2	2.40	0.568	0.0017	0.6713	0.0188	0.0844	0.0008	483	45	521	11	522	5
3	383	1190	115	3.11	0.0589	0.0021	0.6963	0.0231	0.0852	0.0008	562	56	537	14	527	5
4	448	1187	116	2.65	0.0566	0.0016	0.6655	0.0186	0.0847	0.0008	477	44	518	11	524	5
5	404	979	97.1	2.42	0.0561	0.0014	0.6653	0.0167	0.0856	0.0008	454	39	518	10	529	5
6	384	735	74.0	1.92	0.0564	0.0016	0.6598	0.0179	0.0845	0.0007	467	45	514	11	523	4
7	764	1007	107	1.32	0.0578	0.0015	0.6755	0.0182	0.0842	0.0008	522	42	524	11	521	5
8	784	1962	190	2.50	0.0570	0.0013	0.6786	0.0158	0.0859	0.0007	490	42	525	11	531	5
9	358	936	90.6	2.61	0.0569	0.0015	0.6774	0.0181	0.0859	0.0008	486	42	525	11	531	5
10	112	251	25	2.25	0.0577	0.0030	0.6689	0.0343	0.0846	0.0013	518	86	520	21	524	8
11	439	903	90.0	2.06	0.0571	0.0017	0.6721	0.0200	0.0850	0.0009	495	47	522	12	526	5
12	877	1490	153	1.70	0.0573	0.0014	0.6759	0.0160	0.0853	0.0008	502	36	524	10	528	5

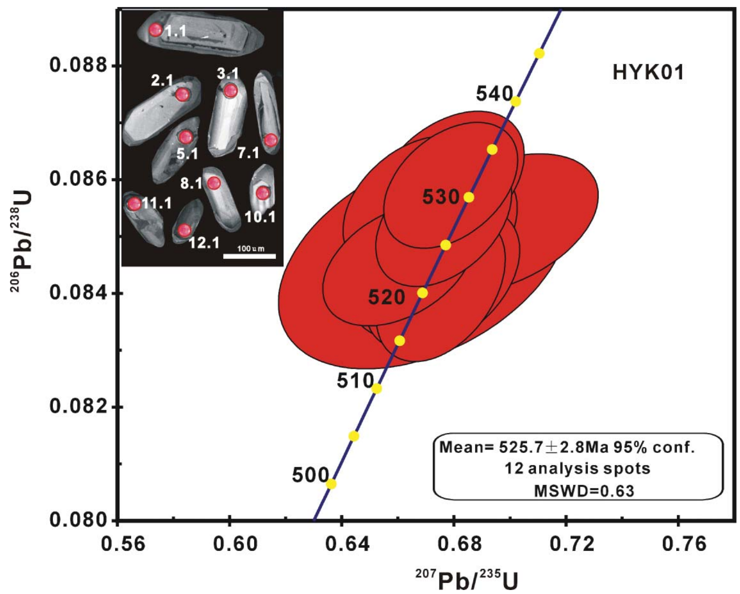

Figure 3. LA-ICP-MS zircon U–Pb concordia diagrams for the nepheline syenites from Zijinshan, Shanxi Province.

GBPG-1 indicated a precision generally better than 5% for all elements. Analyses of the international standards OU-6 and GBPG-1 were in close agreement with recommended values (Table 3).

For analyses of Rb–Sr and Sm–Nd isotopes, sample powders were spiked with mixed isotope tracers, dissolved in Teflon capsules with HF + HNO_3 acids, and separated by conventional cation-exchange techniques. Isotopic measurements were performed on a Finnigan Triton Ti thermal ionization mass spectrometer at the State Key Laboratory of Ore Deposit Geochemistry, Institute of Geochemistry, CAS, Guiyang. Procedural blanks were <200 pg for Sm and Nd and <500 pg for Rb and Sr. Mass fractionation corrections for Sr and Nd isotopic ratios were based on $^{86}Sr/^{88}Sr = 0.1194$ and $^{146}Nd/^{144}Nd = 0.7219$, respectively. Analyses of standards during the period of analysis yielded the following results: NBS987 gave $^{87}Sr/^{86}Sr = 0.710246 \pm 16\ (2\sigma)$ and La Jolla gave $^{143}Nd/^{144}Nd = 0.511863 \pm 8\ (2\sigma)$. The analytical results for Sr–Nd isotopes are presented in Table 4.

4. Results

4.1. LA-ICP-MS U–Pb age determinations

Euhedral zircon grains in samples HYK01 are clean and prismatic, with magmatic oscillatory zoning. Twelve grains gave a weighted mean $^{206}Pb/^{238}U$ age of 525.7± 2.8 Ma (1σ) (95% confidence interval) for HYK01 (Table 1; Figure 3). These determinations are the best estimates of the crystallization ages of the nepheline syenites. In addition, no inherited zircon characteristics are observed.

4.2. Major and trace elements

Tables 2 and 3 show representative whole-rock major and trace element data for the studied nepheline syenites, which have high SiO_2 (59–61 wt.%), Al_2O_3 (20.4–21 wt.%), Na_2O (8.3–9.6 wt.%), and K_2O (5.4–5.6 wt.%) contents, and low Fe_2O_3 (1.73–1.95 wt.%), MgO (0.06–0.11 wt.%, $Mg^{\#}$ = 6.9–11), CaO (0.67–0.83 wt.%), and P_2O_5 (0.001–0.003 wt.%) contents.

In a plot of alkalis (Na_2O + K_2O) versus SiO_2 (Figure 4A), the nepheline syenites plot in the fields of the foid syenite series. In K_2O versus SiO_2 plots (Figure 4B), the syenites plot in the shoshonitic fields. In a plot of the molar ratios of $Al_2O_3/(Na_2O + K_2O)$ and $Al_2O_3/(CaO + Na_2O + K_2O)$, the rocks are mostly peraluminous; some samples fall between the boundary of metaluminous and peralkaline rocks (Figure 4C).

All of the samples show high light rare earth elements [e.g. $(La/Yb)_N$ = 29.1–36.1] (Table 3; Figure 7A), as well as high contents of Rb (226–255 ppm), Th (81.8–93 ppm), U (18.2–21.3 ppm), Pb (48.3–55 ppm), Zr (1240–1370 ppm), and Hf (24.3–26.8 ppm) (Table 3; Figure 7B). All the nepheline syenites have negative Eu anomalies (Eu/Eu^* = 0.5–0.6) (Table 3; Figure 7A). In a primitive mantle-normalized trace elemental diagram, the nepheline syenites are characterized by enrichment in Rb, Th, U, Pb, Zr, and Hf, and depletion in Ba and high field strength elements (Sr, P, and Ti) (Figure 7B). The nepheline syenites show regular trends of increasing Al_2O_3 and CaO, slight decreasing Zr with increasing SiO_2 (Figures 6B, 5E, and 6E). There are no apparent correlations, however, between other oxides, trace elements, and SiO_2 (Figures 6 and 7).

Table 2. Whole-rock major element compositions (wt.%) of representative nepheline syenites from Zijinshan, Shanxi Province.

Sample	Rock type	SiO_2	Al_2O_3	Fe_2O_3	MgO	CaO	Na_2O	K_2O	MnO	P_2O_5	TiO_2	LOI	Total	$Mg^{\#}$	Na_2O+K_2O	T_{zr} (°C)
HYK-1	Nepheline syenite	60.12	20.98	1.95	0.11	0.83	8.78	5.52	0.21	0.002	0.17	1.96	100.64	11	14.3	1045
HYK-2	Nepheline syenite	59.55	20.78	1.74	0.07	0.68	9.44	5.60	0.21	0.001	0.16	2.15	100.38	8.1	15.0	1042
HYK-3	Nepheline syenite	59.49	20.77	1.76	0.06	0.71	9.73	5.42	0.22	0.002	0.16	2.08	100.40	7.0	15.2	1037
HYK-4	Nepheline syenite	59.31	20.50	1.73	0.08	0.78	9.08	5.51	0.21	0.003	0.16	2.29	99.65	9.2	14.6	1032
HYK-5	Nepheline syenite	60.15	20.096	1.78	0.07	0.71	9.07	5.69	0.22	0.001	0.16	1.86	100.58	8.0	14.7	1042
HYK-6	Nepheline syenite	60.44	20.86	1.85	0.10	0.74	8.39	5.57	0.21	0.002	0.16	1.88	100.20	11	14.0	1056
HYK-7	Nepheline syenite	59.91	20.79	1.78	0.08	0.71	9.31	5.55	0.22	0.001	0.16	1.98	100.48	9.0	14.9	1043
HYK-8	Nepheline syenite	59.32	20.47	1.77	0.06	0.68	9.08	5.44	0.22	0.002	0.16	2.32	99.52	6.9	14.5	1048
HYK-9	Nepheline syenite	59.26	20.62	1.76	0.08	0.72	9.35	5.46	0.21	0.003	0.17	1.96	99.59	9.1	14.8	1044
HYK-10	Nepheline syenite	59.53	20.53	1.75	0.06	0.73	9.42	5.51	0.22	0.001	0.16	1.72	99.63	7.0	14.9	1038
HYK-11	Nepheline syenite	59.56	20.51	1.73	0.07	0.75	9.29	5.58	0.23	0.001	0.17	1.76	99.65	8.2	14.9	1041
HYK-12	Nepheline syenite	59.52	20.46	1.74	0.08	0.78	9.36	5.58	0.24	0.002	0.16	1.68	99.60	9.2	14.9	1037
HYK-13	Nepheline syenite	60.13	20.93	1.83	0.09	0.82	8.95	5.54	0.21	0.002	0.16	1.93	100.59	9.8	14.5	1049
HYK-14	Nepheline syenite	59.63	20.74	1.73	0.06	0.67	9.51	5.61	0.22	0.001	0.16	1.98	100.31	7.1	15.1	1037
HYK-15	Nepheline syenite	60.16	20.93	1.76	0.07	0.72	9.06	5.56	0.21	0.001	0.16	1.92	100.55	8.0	14.6	1050
GSR-3	RV*	44.64	13.83	13.4	7.77	8.81	3.38	2.32	0.17	0.95	2.37	2.24	99.88			
GSR-3	MV*	44.75	14.14	13.35	7.74	8.82	3.18	2.3	0.16	0.97	2.36	2.12	99.89			
GSR-1	RV*	72.83	13.4	2.14	0.42	1.55	3.13	5.01	0.06	0.09	0.29	0.7	99.62			
GSR-1	MV*	72.65	13.52	2.18	0.46	1.56	3.15	5.03	0.06	0.11	0.29	0.69	99.70			

Notes: LOI, loss on ignition; $Mg^{\#} = 100 \times Mg/(Mg + \sum Fe)$ atomic ratio; RV*, recommended values; MV*, measured values; values for GSR-1 and GSR-3 are from Wang *et al*. (2003).

Table 3. Trace element contents (ppm) of representative nepheline syenites from Zijinshan, Shanxi Province.

Sample	HYK-1	HYK-2	HYK-3	HYK-4	HYK-5	HYK-6	HYK-7	HYK-8	HYK-9	HYK-10	HYK-11	HYK-12	HYK-13	HYK-14	HYK-15	OU-6 (RV*)	OU-6 (MV*)	GBPG-1 (RV*)	GBPG-1 (MV*)
Sc	1.41	1.54	3.24	1.89	1.21	2.97	1.82	2.84	1.58	1.65	1.84	1.47	2.63	3.12	2.71	22.1	21.6	13.9	14.2
V	7.97	6.38	5.87	5.89	5.98	6.59	6.26	6.34	6.43	6.28	6.31	8.12	6.24	5.76	6.27	129	131	96.5	103
Cr	5.90	0.12	0.41	0.17	0.34	0.94	0.67	0.35	0.14	0.58	0.15	6.05	0.31	0.36	0.29	70.8	73.5	181	187
Ni	2.16	0.42	0.57	1.37	0.61	0.38	0.50	0.45	0.53	1.22	1.34	2.08	0.31	0.52	0.39	39.8	42.5	59.6	60.6
Rb	235	243	236	233	241	253	247	251	255	226	232	243	238	221	243	120	122	56.2	61.4
Sr	8.43	8.55	8.64	8.63	8.72	11.2	7.84	8.76	12.2	8.26	7.78	8.64	8.47	9.89	8.48	131	136	364	377
Y	27.4	26.4	23.6	22.9	26.6	28.2	24.7	25.9	27.4	23.5	21.6	28.3	25.2	22.8	25.6	27.4	26.2	18.0	17.2
Zr	1300	1340	1310	1240	1290	1370	1330	1380	1365	1315	1340	1316	1360	1300	1370	174	183	0.4	0.5
Nb	247	248	238	232	242	252	246	253	258	227	241	254	246	277	245	14.8	15.3	908	921
Ba	6.57	12.1	17.2	18.7	13.8	9.79	8.27	9.17	13.5	7.86	8.33	7.11	9.54	15.9	8.84	477	486	18.6	20.9
Ga	39.2	36.0	31.5	32.3	38.5	40.1	31.4	32.7	37.3	30.5	31.7	40.6	31.4	30.7	31.8	24.3	26.5	18.6	20.9
La	163	161	154	152	157	170	158	164	168	173	164	166	151	146	157	33.0	33.1	103	105
Ce	212	210	200	202	206	223	207	215	221	192	216	224	208	187	206	74.4	78.0	11.5	11.6
Pr	16.9	16.6	15.7	15.7	16.4	17.6	16.2	16.8	17.2	17.8	16.6	17.4	15.6	15.2	15.9	7.8	8.1	43.3	42.4
Nd	35.9	36.6	33.4	33.9	34.4	36.7	34.4	35.6	35.4	33.5	34.8	36.3	34.7	32.8	34.6	29.0	30.6	6.8	6.6
Sm	4.07	4.08	3.75	3.89	3.78	4.22	3.75	3.96	4.17	3.66	3.83	4.13	3.82	3.63	3.79	5.92	5.99	1.79	1.69
Eu	0.63	0.60	0.59	0.60	0.63	0.67	0.60	0.62	0.66	0.54	0.64	0.68	0.57	0.53	0.55	1.36	1.35	4.74	4.47
Gd	3.31	3.29	3.04	2.83	3.19	3.21	3.16	3.34	3.35	3.12	3.23	3.37	3.08	2.91	3.13	5.27	5.50	0.60	0.59
Tb	0.49	0.49	0.44	0.43	0.47	0.48	0.45	0.48	0.52	0.41	0.48	0.53	0.45	0.42	0.46	0.85	0.83	3.26	3.17
Dy	3.23	3.22	2.88	2.77	3.15	3.26	3.01	3.26	3.28	2.95	3.06	3.29	3.14	2.81	3.22	4.99	5.06	0.69	0.66
Ho	0.79	0.82	0.73	0.70	0.76	0.79	0.76	0.74	0.85	0.72	0.75	0.81	0.71	0.72	0.73	1.01	1.02	2.01	2.02
Er	2.95	0.87	2.46	2.49	2.75	2.80	2.57	2.70	2.93	2.48	2.64	3.05	2.63	2.41	2.66	2.98	3.07	0.30	0.29
Tm	0.50	0.51	0.46	0.44	0.50	0.48	0.43	0.49	0.54	0.41	0.45	0.52	0.44	0.43	0.47	0.44	0.45	2.03	2.03
Yb	4.02	3.96	3.32	3.41	3.74	3.94	3.58	3.70	4.05	3.44	3.63	4.06	3.62	3.25	3.65	3.00	3.09	0.31	0.31
Lu	0.66	0.61	0.51	0.53	0.59	0.61	0.57	0.61	0.63	0.51	0.62	0.68	0.57	0.48	0.59	0.45	0.47	6.07	5.93
Hf	25.3	26.6	25.5	24.3	25.4	26.2	25.6	26.0	26.8	24.5	25.9	25.7	25.3	24.7	25.8	4.7	4.9	232	224
Ta	11.5	11.5	10.9	11.2	11.2	11.8	11.2	11.3	12.2	10.8	11.5	11.6	10.8	10.5	11.1	1.1	1.0	14.1	14.5
Pb	53.1	52.8	49.8	48.3	51.0	55.0	51.4	54.3	54.5	50.4	50.6	54.3	52.7	48.3	53.6	28.2	32.7	11.2	11.4
Th	89.9	88.9	85.9	81.8	87.5	95.0	87.9	93.0	90.2	86.3	89.5	92.4	89.6	83.7	92.1	11.5	13.9	11.2	11.4
U	19.0	19.3	19.7	18.2	18.7	20.5	19.3	20.7	21.3	18.4	20.6	20.8	18.5	18.8	19.3	1.96	2.19	0.90	0.99
$^{\delta}$Eu	0.5	0.5	0.5	0.6	0.6	0.6	0.5	0.5	0.5	0.5	0.6	0.6	0.5	0.5	0.5				
$(La/Yb)_N$	29.1	29.2	33.3	32.9	30.01	30.9	31.7	31.8	29.8	36.1	32.4	29.3	29.9	32.2	30.9				

Notes: RV*, recommended values; MV*, measured values. Values for GBPG-1 are from Thompson *et al*. (2000); those for OU-6 are from Potts and Kane (2005).

Table 4. Sr–Nd isotopic compositions of the nepheline syenites in Zijinshan, Shanxi Province.

Sample	Age(Ma)	Sm(ppm)	Nd(ppm)	Rb(ppm)	Sr(ppm)	$^{87}Rb/^{86}Sr$	$^{87}Sr/^{86}Sr$	2σ	$(^{87}Sr/^{86}Sr)_i$	$^{147}Sm/^{144}Nd$	$^{143}Nd/^{144}Nd$	2σ	$(^{143}Nd/^{144}Nd)_i$	$\epsilon_{Nd}(t)$
HYK-1		4.07	35.9	235	8.43	80.5635	1.307874	8	0.704222	0.0891	0.512306	10	0.511999	0.8
HYK-2		4.08	36.6	243	8.55	82.1368	1.319685	10	0.704244	0.0674	0.5122235	8	0.512003	0.8
HYK-3		3.75	33.4	236	8.64	78.9398	1.295725	12	0.704239	0.0679	0.512231	8	0.511997	0.7
HYK-5	525.7	3.78	34.4	241	8.72	79.8727	1.302721	10	0.704245	0.0664	0.512231	10	0.512002	0.8
HYK-8		3.96	35.65	251	8.76	82.8071	1.324695	12	0.704232	0.0672	0.512232	8	0.512000	0.8
HYK-10		3.66	33.5	226	8.26	79.0726	1.296722	8	0.704241	0.0660	0.512224	10	0.511997	0.7
HYK-12		4.13	36.3	243	8.64	81.2813	1.323268	10	0.704238	0.0688	0.512238	8	0.512001	0.8
HYK-15		3.79	34.6	243	8.48	82.8149	1.32477	12	0.704248	0.0662	0.512230	8	0.512002	0.8

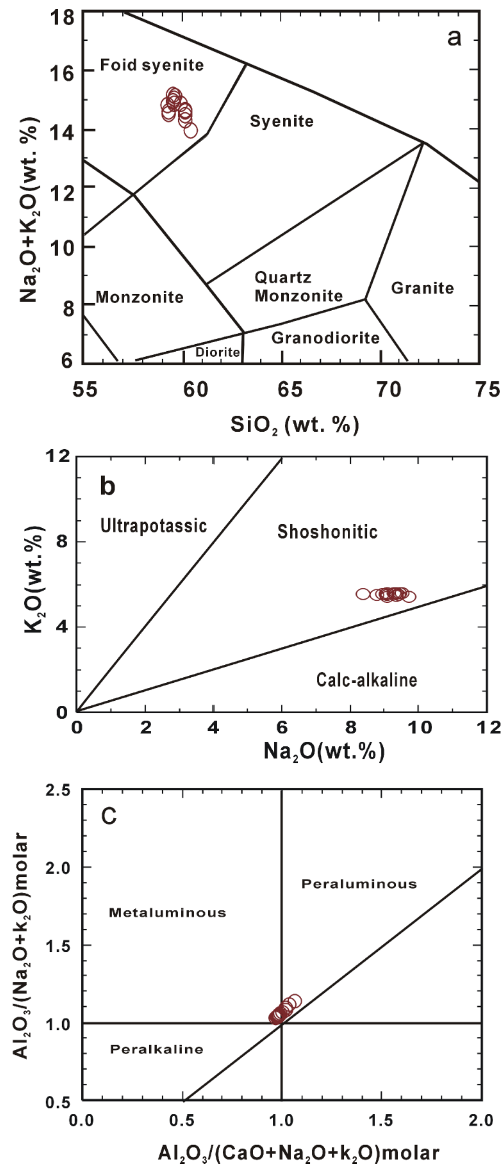

Figure 4. Whole-rock (A) SiO_2 versus $Na_2O + K_2O$, (B) Na_2O versus K_2O, and (C) $Al_2O_3/(CaO + Na_2O + K_2O)$ molar versus $Al_2O_3/(Na_2O + K_2O)$ molar for the nepheline syenites from Zijishan.

4.3. Sr–Nd isotopes

Sr and Nd isotopic data for representative samples of the nepheline syenites (Table 4; Figure 8) yield low ranges in $(^{87}Sr/^{86}Sr)_i$ values (0.7042–0.7043) and positive initial ε_{Nd} (t) values (0.7–0.8), indicating a compositionally depleted source.

5. Discussion

5.1. Crustal contamination

The nepheline syenite is characterized by marked positive Pb anomalies on a multi-element normalized spidergram

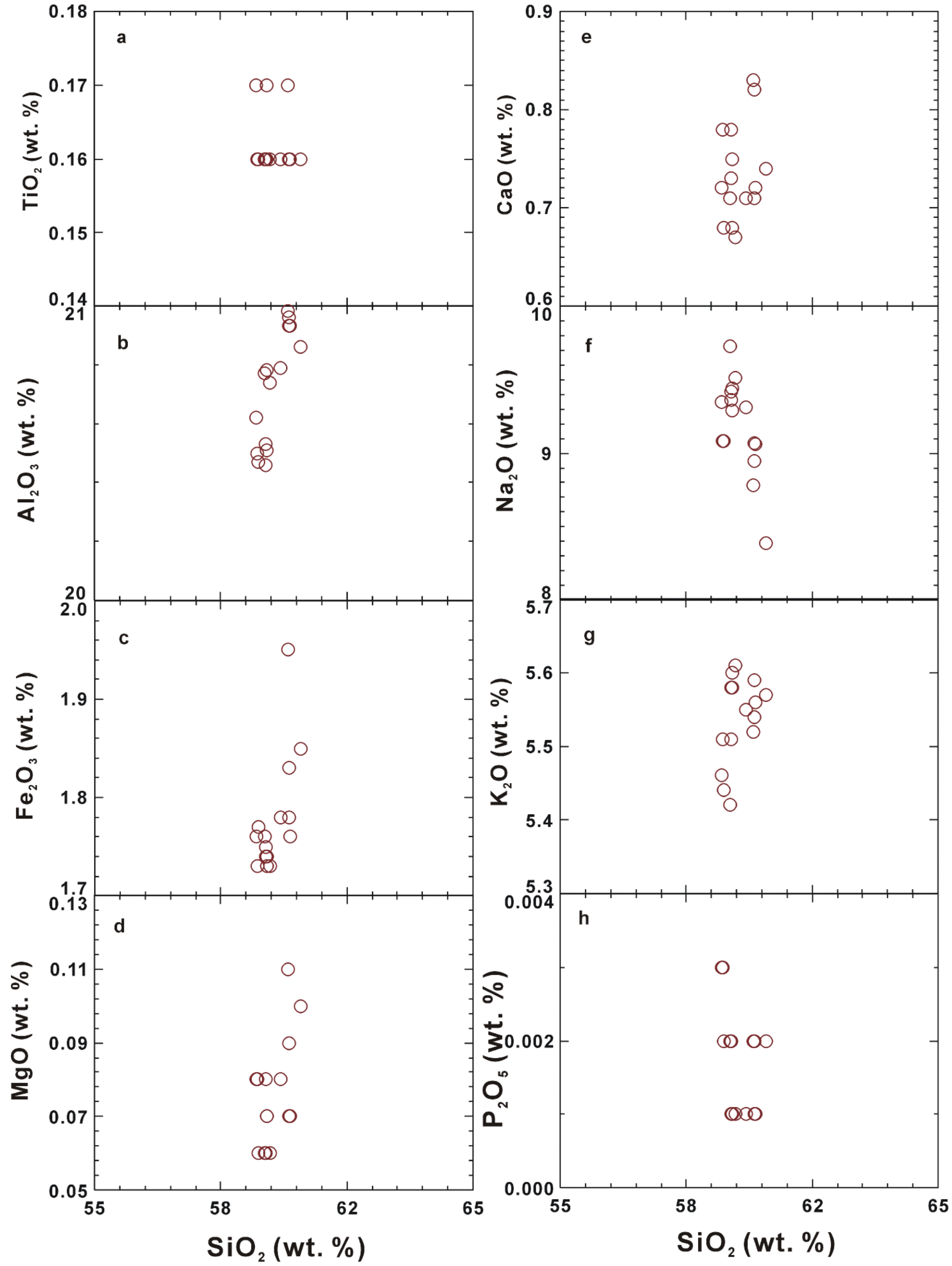

Figure 5. Whole-rock SiO_2 versus SiO_2, TiO_2, Al_2O_3, Fe_2O_3, MgO, CaO, Na_2O, K_2O, and P_2O_5 for the nepheline syenites from Zijinshan, Shanxi Province.

(Figure 7B), which is consistent with the involvement of crustal compositions (Rudnick and Fountain 1995). In combined studies of chondrite-normalized REE diagrams (Figure 7A), some of the trace element contents and ratios, for example, Th, Pb, and Eu/Eu*, indicate that an upper crustal component, but not the middle–lower crust, is involved in the generation of the nepheline syenites (Rudnick and Fountain 1995). The peraluminous, silica-rich composition of the nepheline syenite further suggests an important contribution of metasedimentary material among its sources. The lack of correlation between the ε_{Nd} (t) values and Nd concentrations for the nepheline syenite (Figure 8B), however, precludes assimilation and fractional crystallization as a major process during the late evolutionary stages, at a shallow crustal level. The granitoid rocks have low initial $^{87}Sr/^{86}Sr$ ratios (0.7042–0.7043) and slightly positive ε_{Nd} (t) values (0.7–0.8) (Table 4; Figure 8A). Therefore, the geochemical

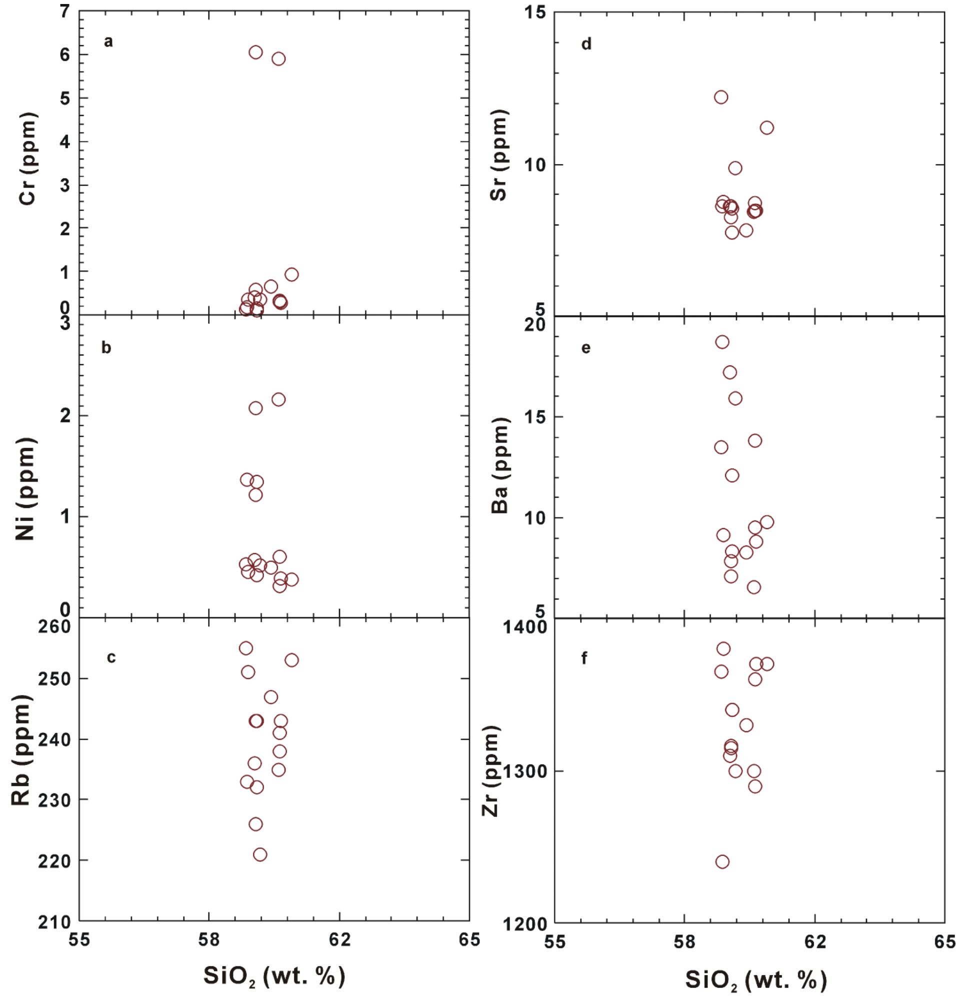

Figure 6. Whole-rock SiO_2 versus Cr, Ni, Rb, Sr, Ba, and Zr for the nepheline syenites from Zijinshan.

and Sr–Nd isotopic signatures of the nepheline syenites are mainly inherited from a depleted source.

5.2. *Fractional crystallization*

The variable $Mg^{\#}$ (6.9–11) and low element content, such as Cr (0.12–6.05 ppm) and Ni (0.31–2.16 ppm) (Table 3), of the nepheline syenite are consistent with slight fractionation. For the studied nepheline syenites, Al_2O_3 and CaO show a positive correlation with SiO_2 (Figure 6B and 6E), which is probably related to the fractionation of plagioclase. Plagioclase fractional crystallization is further supported by the negative Eu and Sr anomalies observed in the studied nepheline syenites (Figure 7A and 7B). In addition, the presence of negative P and Ti anomalies in the analysed samples (Figure 7B) supports the fractionation of Ti-bearing oxides (e.g. rutile, ilmenite, and titanite) and apatite.

The nepheline syenites show slightly decreasing Zr with increasing SiO_2 (Figure 6F), indicating that zircon was relatively saturated in the magma and was also a major fractionating phase controlled by fractional crystallization (Li *et al*. 2007). Zircon saturation thermometry (Watson and Harrison 1983) provides a simple and robust means of estimating magma temperatures from bulk-rock compositions. The calculated zircon saturation temperatures (T_{Zr}) of the nepheline syenites were 1032–1056°C (Table 2), representing the crystallization temperature of the magma.

5.3. *The source and petrogenetic model*

The high silica contents (59.26–60.44 wt.%), relatively low concentrations of MgO (0.06–0.11 wt.%, or $Mg^{\#}$ s), Cr (0.12–6.05 ppm), Ni (0.31–2.16 ppm), and $^{87}Sr/^{86}Sr$ (0.7042–0.7043), and positive ε_{Nd} (t) (0.7–0.8) suggest that the nepheline syenites were derived by crustal assimilation and fractional crystallization, or from a felsic rather than mafic–ultramafic source. The lack of crust assimilation, however, precludes the first probability. Crustal rocks can be recommended as possible sources because experimental evidence shows that partial melting of any

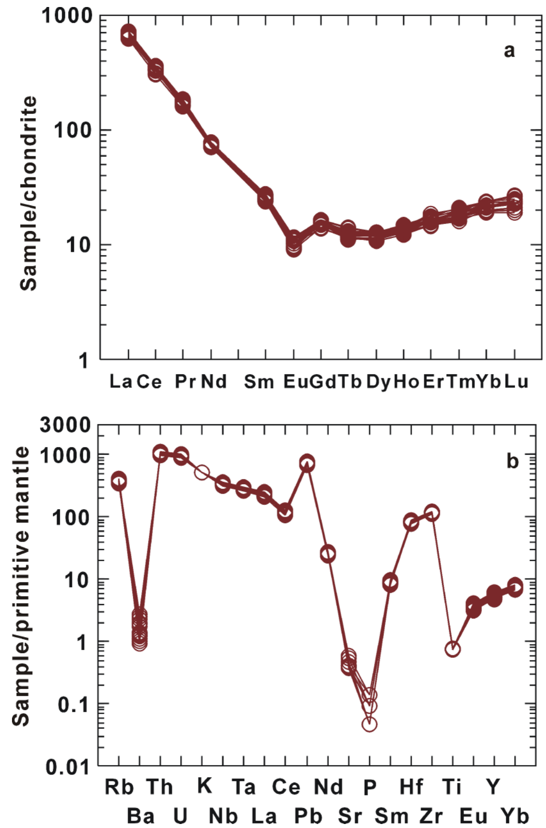

Figure 7. Whole-rock (A) chondrite-normalized rare earth element patterns and (B) primitive mantle-normalized spider diagrams of the nepheline syenites from Zijinshan. Primitive mantle and chondritic abundances are from Sun and McDonough (1989).

of the older, exposed crustal rocks (e.g. Hirajima *et al*. 1990; Yang *et al*. 1993; Zhang *et al*. 1994, 1995; Kato *et al*. 1997) and lower crustal intermediate granulites (Gao *et al*. 1998a, b) in the deep crust would produce high-Si, low-Mg liquids (i.e. granitoid liquids; Rapp *et al*. 2003), as the nepheline syenite magmas present in the Shanxi alkaline rocks. Moreover, the Sr–Nd isotopic signatures of the nepheline syenites are incomparable with the associated and homochronous mafic dikes in the study area in terms of favouring their derivation from felsic magmas and are non-similar to the parental magmas of the mafic rocks in the mantle source.

At present, models proposed for the generation of syenites may be divided into three groups. First, syenite magmas may originate by partial melting of crustal rocks resulting from an influx of volatiles (e.g. Lubala *et al*. 1994) or in a closed system at pressures typical of the base of over-thickened crust (Huang and Wyllie 1981). Second, syenite magmas may be products of partial melting of metasomatized mantle (Sutcliffe *et al*. 1990; Lynch *et al*. 1993) or the residual melts formed by differentiation of alkali basalt magma (Parker 1983; Brown and Becker 1986; Thorpe and Tindle 1992). Third, syenites may result from magma mixing processes, particularly mixing of basic and silicic melts with subsequent differentiation of the hybrid liquids (Barker *et al*. 1975; Sheppard 1995; Zhao *et al*. 1995; Litvinovsky *et al*. 2002) or by mixing of mantle-derived, silica-undersaturated alkaline magmas with lower crustally derived granitic magmas (e.g. Dorais 1990).

Several extensive studies on the Mesozoic alkaline complex in Zijishan, Shanxi Province, have been conducted. For example, Liu (2008) previously studied Zijinshan alkaline complexes (including some nepheline syenites) and suggested that petrogenesis is related to WN-trending subduction and extrusion of the Pacific block. The activity of the Pacific block extends to middle and western China and yields a large-scale alkaline complex in Zijinshan. The petrogenetic model is mainly due to magma mixing. Yang *et al.* (2009) investigated some Zijinshan alkaline rocks in Shanxi Province; they proposed that the formation of alkaline rocks could be attributed to asthenospheric upwelling, which triggers alkaline magmatism, tectonic transformations, lithosphere thinning, underplating of the mantle magma, and tectonothermal events within Shandong Province and the NCC. In addition, Ying *et al.* (2007) considered that the Zijinshan alkaline complex is generated in an extensional environment. Nevertheless, detailed research on the Palaeozoic alkaline rocks in Zijinshan, Shanxi Province, has not been conducted on

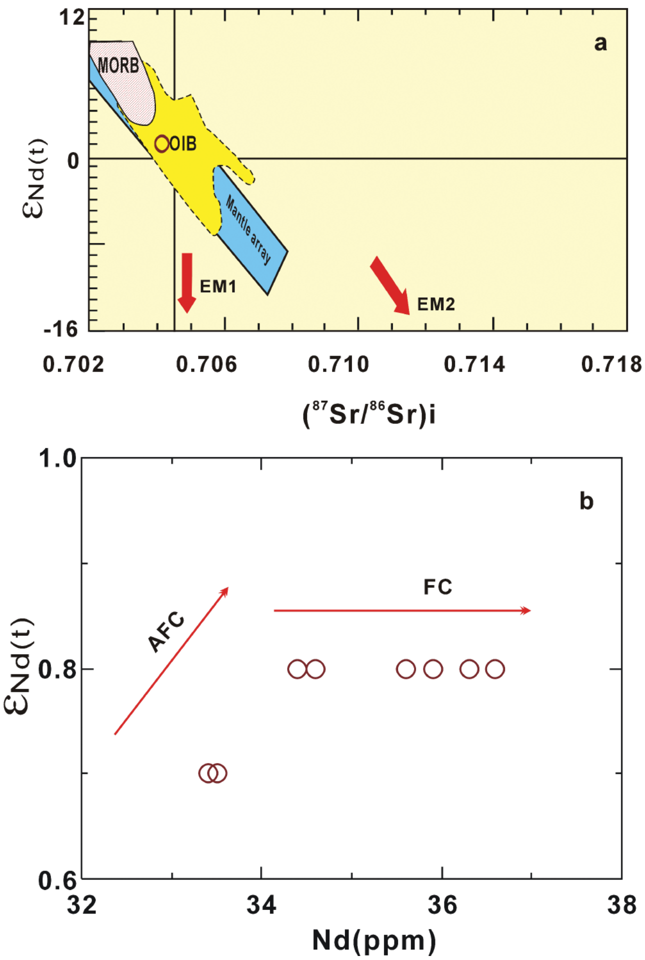

Figure 8. Whole-rock (A) $(^{87}Sr/^{86}Sr)_i$ versus ε_{Nd} (t); and (B) Nd versus ε_{Nd} (t) for the nepheline syenite from Zijinshan, Shanxi Province.

the basis of the above discussions. Nepheline syenites do not appear to be derived from mantle sources, which directly preclude the second and third models. We thus prefer the first model to interpret the petrogenesis of the nepheline syenites, specifically, nepheline syenite magmas originating from the partial melting of crustal rocks.

6. Conclusions

Based on the geochronological, geochemical, and Sr–Nd isotopic data, the following conclusions concerning the origins of the nepheline syenites can be drawn.

(1) The U–Pb zircon age data indicate that the studied Zijinshan nepheline syenites crystallized at 525.7 ± 2.8 Ma.

(2) The nepheline syenites belong to the foid syenite magma series and show shoshonitic whole-rock affinities based on their K_2O and Na_2O contents. The rocks have high light rare earth elements [$(La/Yb)_N = 29.1–36.1$], show negative Eu anomalies ($\delta Eu = 0.5–0.6$), positive anomalies in Rb, Th, U, Pb, Zr, and Hf, and are depleted in Ba and high field strength elements (P and Ti). The studied rocks all show relatively low radiogenic Sr $(^{87}Sr/^{86}Sr)_i$ (0.7042–0.7043) and positive ε_{Nd} (t) (0.7–0.8), suggesting origination from a depleted felsic crust source.

(3) The parent magmas probably originated via fractional crystallization of plagioclase and Fe–Ti oxides (e.g. rutile, ilmenite, titanite, etc.), apatite, and zircon during the ascent of alkaline rocks with negligible crustal contamination. Zircon saturation temperatures (T_{Zr}) of the felsic rocks are 1032–1056°C, approximately representing the crystallization temperature of the alkaline magma.

Acknowledgements

This research was supported by the National Nature Science Foundation of China (Grant Nos. 40773020, 40972071, 40673029, 90714010, and 40634020). We are grateful to Xiaobiao Li for helping with the analyses of Sr and Nd isotopes, and Yongsheng Liu and Zhaochu Hu for their assistance with the zircon U–Pb dating.

References

Andersen, T., 2002, Correction of common lead in U–Pb analyses that do not report ^{204}Pb: Chemical Geology, v. 192, p. 59–79.
Barker, F., Wones, D.R., Sharp, W.N., and Desborough, G.A., 1975, The Pikes Peak batholith, Colorado Front Range, and a model for the origin of the abbro-anorthosite-syenite-potassic granite suite: Precambrian Research, v. 2, p. 97–160.
Brown, P.E., and Becker, S.M., 1986, Fractionation, hybridisation and magma-mixing in the Kialineq centre East Greenland: Contributions to Mineralogy and Petrology, v. 92, p. 57–70.
Burat, F., Kangal, O., and Guyen, 2006, An alternative mineral in the glass and ceramic industry: Nepheline syenite: Minerals Engineering, v. 19, p. 370–371.
Dorais, M.J., 1990, Compositional variations in pyroxenes and amphiboles of the Belknap Mountain complex, New Hampshire: Evidence for origin of iliac-saturated alkaline rocks: The American Mineralogist, v. 75, p. 1092–1105.
Esposito, L., Salem, A., Tucci, A., Gualtieri, A., and Jazayeri, S.H., 2005, The use of nepheline-syenite in a body mix for porcelain stoneware tiles: Ceramic International, v. 31, p. 233–240.
Gao, S., Luo, T.-C., Zhang, B.-R., Zhang, H.-F., Han, Y.-W., Zhao, Z.-D., and Hu, -K., 1998a, Chemical composition of the continental crust as revealed by studies in East China: Geochimica et Cosmochimica Acta, v. 62, p. 1959–1975.
Gao, S., Zhang, B.-R., Jin, Z.-M., Kern, H., Luo, T.-C., and Zhao, Z.-D., 1998b, How mafic is the lower continental crust?: Earth and Planetary Science Letters, v. 106, p. 101–117.
Hirajima, T., Ishiwatari, A., Cong, B., Zhang, R., Banno, S., and Nozaka, T., 1990, Coesite from Mengzhong eclogite at Donghai county, northern Jiangsu province, China: Mineralogical Magazine, v. 54, p. 579–583.

Hu, J.Y., and Zhou, A.C., 2007, Geochemical characteristics of Zijinshan alkaline complex in Linxian, Shanxi province: Journal of Taiyuan University of Technology, v. 38, p. 339–343.

Huang, Q., and Qiu, S.M., 2001, Geological features of nepheline syenite in China: Geology and Mineral Resources Research, v. 16, p. 68–72. (in Chinese with English abstract).

Huang, W.L., and Wyllie, P.J., 1981, Phase relationships of S-type granite with H_2O to 35 kbar: Muscovite granite from Harney Peak, South Dakota: Journal of Geophysical Research, v. 86, p. 10515–10529.

Kato, T., Enami, A., and Zhai, M., 1997, Ultrahigh-pressure marble and eclogite in the Su-Lu ultrahigh-pressure terrane, eastern China: Journal of Metamorphic Geology, v. 15, p. 169–182.

Li, X.H., Li, Z.X., Li, W.X., Liu, Y., Yuan, C., Wei, G.J., and Qi, C.S., 2007, U–Pb zircon, geochemical and Sr–Nd–Hf isotopic constraints on age and origin of Jurassic I- and A-type granites from central Guangdong, SE China: A major igneous event in response to foundering of a subducted flat-slab? Lithos, v. 96, p. 186–204.

Litvinovsky, B.A., Jahn, B.M., Zanvilevich, A.N., and Shadaev, M.G., 2002, Crystal fractionation in the petrogenesis of an alkali monzodiorite-syenite series: The Oshurkovo plutonic sheeted complex, Transbaikalia, Russia: Lithos, v. 64, p. 97–130.

Liu, D., 2008. Geochemical characteristics of the Zijinshan alkaline complex in Linxian, Shanxi province: Tiayuan: Tiayuan University of Technology (in Chinese).

Lubala, R.T., Frick, C., Roders, J.H., and Walraven, F., 1994, Petrogenesis of syenites and granites of the Schiel Alkaline complex, Northern Transvaal, South Africa: Journal of Geology, v. 102, p. 307–309.

Ludwig, K.R., 2003, User's manual for Isoplot/Ex, Version 3.00: A geochronological toolkit for Microsoft Excel: Berkeley Geochronology Center Special Publication 4, p. 1–70.

Lynch, D.J., Musselman, T.E., Gutmann, J.T., and Patchett, P.J., 1993, Isotopic evidence for the origin of Cenozoic volcanic rocks in the Pinacate volcanic field, Northwestern Mexico: Lithos, v. 29, p. 295–302.

Nepheline Syenite Inventory, 1999, Nepheline Syenite. özpeker Istanbul I. (Ed.), Mineral and Metals Exporters Association, December 1999, p. 10–30 (in Turkish).

Parker, D.F., 1983, Origin of the trachyte-quartz trachyte-peralkalic rhyolite suite of the Oligocene Paisano volcano, Trana-Pecos Texas: Geological Society of America Bulletin, v. 94, p. 614–629.

Potts, P.J., and Kane, J.S., 2005, International association of geoanalysts certificate of analysis: Certified reference material OU-6 (Penrhyn slate): Geostandards and Geoanalytical Research, v. 29, p. 233–236.

Qi, L., Hu, J., and Grégoire, D.C., 2000, Determination of trace elements in granites by inductively coupled plasma mass spectrometry: Talanta, v. 51, p. 507–513.

Rapp, R.P., Shimizu, N., and Norman, M.D., 2003, Growth of early continental crust by partial melting of eclogite: Nature, v. 425, p. 605–609.

Rudnick, R.L., and Fountain, D.M., 1995, Nature and composition of the continental crust: A lower crustal perspective: Reviews of Geophysics, v. 33, p. 267–309.

Sheppard, S., 1995, Hybridization of shoshonitic lamprophyre and calc-alkaline granite magma in the early Proterozoic Mt. Bundey igneous suite, Northern Territory: Australian Journal of Earth Sciences, v. 42, p. 173–185.

Sun, S.S., and McDonough, W.F., 1989, Chemical and isotopic systematics of oceanic basalts: Implications for mantle composition and processes, in Saunders, A.D., and Norry, M.J., eds., Magmatism in the Ocean Basins: Geological Society Special Publication, p. 313–345.

Sutcliffe, R.H., Smith, A.R., Doherty, W., and Barnett, R.L., 1990, Mantle derivation of Archean amphibole-bearing granitoids and associated mafic rocks: Evidence from the southern Superior Province, Canada: Contributions to Mineralogy and Petrology, v. 105, p. 255–274.

Tait, K.T., Sokolova, E., Hawthorne, F.C., and Khomyakov, A.P., 2003, The crystal chemistry of nepheline: Canadian Mineralogist, v. 41, p. 61–70.

Thompson, M., Potts, P.J., Kane, J.S., and Wilson, S., 2000, An international proficiency test for analytical geochemistry laboratories-report on round 5 (August 1999): Geostandards and Geoanalytical Research, v. 24, p. E1–E28.

Thorpe, R.S., and Tindle, A.G., 1992, Petrology and petrogenesis of a Tertiary modal dolerite-peralkaline/subalkaline-trachyte/rhyolite dyke association from Lundy, Bristol Channel, UK: The Journal of Geology, v. 27, p. 101–117.

Wang, Y.M., Gao, Y.S., Han, H.M., and Wang, X.H., 2003, Practical handbook of reference materials for geoanalysis: Geological Publishing House, p. 16–23. (in Chinese).

Watson, E.B., and Harrison, T.M., 1983, Zircon saturation revisited: temperature and composition effects in a variety of crustal magma types: Earth and Planetary Science Letters, v. 64, p. 295–304.

Yang, J., Godard, G., Kienast, J.R., Lu, Y., and Sun, J., 1993, Ultrahighpressure 60 kbar magnesite-bearing garnet peridotites from northeastern Jiangsu, China: Journal of Geology, v. 101, p. 541–554.

Yang, X.K., Chao, H.X., Volkova, N.I., Zheng, M.L., and Yao, W.H., 2009, Geochemistry and SHRIMP geochronology of alkaline rocks of the Zijinshan massif in the eastern Ordos basin, China: Russian Geology and Geophysics, v. 50, p. 751–762.

Ying, J.F., Zhang, H.F., Sun, M., Tang, Y.J., Zhou, X.H., and Liu, X.M., 2007, Petrology and geochemistry of Zijinshan alkaline intrusive complex in Shanxi province, western North China Craton: Implication for magma mixing of different sources in an extensional regime: Lithos, v. 98, p. 45–66.

Yuan, H.L., Gao, S., Liu, X.M., Li, H.M., Gunther, D., and Wu, F.Y., 2004, Accurate U–Pb age and trace element determinations of zircon by laser ablation-inductively coupled plasma mass spectrometry: Geostandards Newsletter, v. 28, p. 353–370.

Zhang, R.Y., Hirajima, T., Banno, S., Cong, B., and Liou, J.G., 1995, Petrology of ultrahigh-pressure metamorphic rocks in southern Sulu region, eastern China: Journal of Metamorphic Geology, v. 13, p. 659–675.

Zhang, R.Y., Liou, J.G., and Cong, B., 1994, Petrogenesis of garnetbearing ultramafic rocks and associated eclogites in the SuLu ultrahigh-P metamorphic terrane, astern China: Journal of Metamorphic Geology, v. 12, p. 169–186.

Zhao, J.-X., Shiraishi, K., Ellis, D.J., and Sheraton, J.W., 1995, Geochemical and isotopic studies of syenites from the Yamoto Mountains, East Antartica: Implication for the origin of syenitic magmas: Geochimica et Cosmochimica Acta, v. 59, p. 1363–1385.

Zhao, Z.H., and Zhou, L.D., 1994, Rare earth elements feature of some alkali-enriched intrusions in China: Science in China (B), v. 24, p. 1108–1120.

Zhou, L.D., and Zhao, Z.H., 1994, Pathogenesis and geochemistry of alkali-enriched intrusions in China: Science in China (B), v. 24, p. 1093–1101.

Zhou, L.D., and Zhao, Z.H., 1996, Research on chronology for some alkaline rocks in China: Geochimica, v. 25, p. 164–171.